Received: 30 August 2016 | Accepted: 22 November 2016
DOI 10.1002/hyp.11088

WILEY HP TODAY

SCIENTIFIC BRIEFING

Tropical precipitation anomalies and *d*-excess evolution during El Niño 2014-16

Ricardo Sánchez-Murillo[1] | **Ana M. Durán-Quesada**[2,3] | **Christian Birkel**[4,5] | **Germain Esquivel-Hernández**[1] | **Jan Boll**[6]

[1] Stable Isotope Research Group, National University of Costa Rica, Heredia, Costa Rica
[2] Centre of Geophysical Research, University of Costa Rica, San José, Costa Rica
[3] Department of Atmospheric, Oceanic, and Planetary Physics, School of Physics, University of Costa Rica, San José, Costa Rica
[4] Department of Geography, University of Costa Rica, San José, San José, Costa Rica
[5] Northern Rivers Institute, University of Aberdeen, Aberdeen, AB24 3UF, Aberdeen, Scotland
[6] Department of Civil and Environmental Engineering, Washington State University, Pullman, Washington, USA

Correspondence
Ricardo Sánchez-Murillo, Stable Isotope Research Group, National University of Costa Rica, Campus Omar Dengo, Heredia, Costa Rica, P.O. Box: 86-3000.
Email: ricardo.sanchez.murillo@una.cr

Funding information
International Atomic Energy Agency, Grant/Award Number: CRP-19747; Research Office of the National University of Costa Rica, Grant/Award Number: SIA-0482-13, SIA-0378-14. SIA-0101-14.

Abstract

The last 2014-16 El Niño event was among the three strongest episodes on record. El Niño considerably changes annual and seasonal precipitation across the tropics. Here, we present a unique stable isotope data set of daily precipitation collected in Costa Rica prior to, during, and after El Niño 2014-16, in combination with Lagrangian moisture source and precipitation anomaly diagnostics. δ^2H composition ranged from -129.4 to +18.1 (‰) while δ^{18}O ranged from -17.3 to +1.0 (‰). No significant difference was observed among δ^{18}O (P=0.186) and δ^2H (P=0.664) mean annual compositions. However, mean annual *d-excess* showed a significant decreasing trend (from +13.3 to +8.7 ‰) (P<0.001) with values ranging from +26.6 to -13.9 ‰ prior to and during the El Niño evolution. The latter decrease in *d-excess* can be partly explained by an enhanced moisture flux convergence across the southeastern Caribbean Sea coupled with moisture transport from northern South America by means of an increased Caribbean Low Level Jet regime. During 2014-15, precipitation deficit across the Pacific domain averaged 46% resulting in a very severe drought; while a 94% precipitation surplus was observed in the Caribbean domain. Understanding these regional moisture transport mechanisms during a strong El Niño event may contribute to a) better understanding of precipitation anomalies in the tropics and b) re-evaluate past stable isotope interpretations of ENSO events in paleoclimatic archives within the Central America region.

KEYWORDS

Costa Rica, ENSO, *d*-excess, moisture transport, tropical precipitation

1 | INTRODUCTION

The last El Niño/Southern Oscillation (ENSO) event was catalogued as one of the three strongest events on record (e.g. 1982-83, 1997-98, and 2014-16) according to the Multivariate ENSO Index (MEI) ranking (Wolter & Timlin, 1998). The ENSO Situation Report recently released by the United Nations Food and Agriculture Organization (FAO, 2016) indicated that more than 60 million people worldwide were affected by this ENSO-related droughts, floods, and extreme hot and cold weather. In the Dry Corridor of Central America alone, an area that extends from Chiapas, Mexico to northwestern Costa Rica (Pacific domain), and also includes Panama's "Arco Seco" dry area (Sánchez-Murillo & Birkel, 2016), 3.5 million people experienced food insecurity after suffering major crop losses due to prolonged drought conditions from 2014 to the beginning of 2016 (FAO, 2016).

Future climate scenarios indicate that a distinct drying pattern may affect the precipitation regime in Central America, resulting in significant reductions in median precipitation (5-10%) and runoff (10-30%) depending on location and associated mainly with the occurrence of anomalous dry years (Hidalgo, Amador, Alfaro, & Quesada, 2013). However, seasonal and interannual precipitation forecasting prior to and during warm and cold ENSO phases remains a challenge (Capotondi et al., 2015; Lee et al., 2012), particularly in the tropics (Nicholson, 2014; Cid-Serrano, Ramírez, Alfaro, & Enfield, 2015; Zhang, Yang, Jiang, & Zhao, 2016; Hidayat, Ando, Masumoto, & Luo, 2016; Tedeschi & Collins, 2016). Physically-based global circulation models (GCMs) often have failed to accurately predict precipitation patterns at small scales in the tropics (Kusangaya, Toucher, van Garderen, & Jewitt, 2016). In recent years, water stable isotopes (δ^{18}O and δ^2H) of precipitation and water vapour as well as second-order parameters (e.g. deuterium excess, hereafter *d*-excess=δ^2H-8*δ^{18}O; Dansgaard, 1964), have provided reliable and novel data for evaluating global isotope simulations generated by GCMs (Dittmann et al., 2016; Haese, Werner, & Lohmann, 2013).

Satellite missions such as TES (Tropospheric Emission Spectrometer), SCHIAMACHY (Scanning Imaging Absorption Spectrometer for Atmospheric Cartography), and GOSAT (Greenhouse gases Observing Satellite) have allowed the combination of GCMs, upper air measurements, and stable isotope observations in precipitation and water vapour to characterize moisture transport processes at global and regional scales (Frankenberg et al., 2013; Good, Noone, Kurita, Benetti, & Bowen, 2015; Lee et al., 2012; Midhun & Ramesh, 2016; Payne, Noone, Dudhia, Piccolo, & Grainger, 2007; Sutanto et al., 2015; Yoshimura et al., 2011). Despite the increasing trend in powerful computational analysis and available satellite information, there is still a significant lack of continuous and high frequency (i.e. daily or event-based) stable isotope monitoring for precipitation and water vapour in the tropics (Bershaw, Saylor, Garzione, Leier, & Sundell, 2016; Sánchez-Murillo & Birkel, 2016) that can provide essential information to cross-validate GCMs and satellite measurements of extreme changes in atmospheric circulation, particularly during ENSO cycles (Yoshimura, 2015).

Lately, more attention has been paid to *d*-excess changes in a wide variety of paleoclimatic archives, such as ice cores (Klein et al., 2016), speleothems (Demény et al., 2013), and lake sediments (Hepp et al., 2015) in order to reconstruct source precipitation conditions coupled with subsequent analysis of potential air mass back trajectories (Pfahl & Wernli, 2008; Risi, Landais, Winkler, & Vimeux, 2013). Jouzel et al. (2013) explained that *d*-excess values may deviate from +10 (‰) due to the combination of three factors: a) a relative humidity (RH) increase in the precipitation source, b) a decrease in sea surface temperature (SST), and c) greater wind speeds (>7 ms^{-1}) affecting the evaporation regime and subsequent kinetic fractionation. The authors also emphasize that there is no consensus regarding the sensitivity of precipitation *d*-excess to local temperature as a potential secondary controlling process. Additionally, the recycling of transpiration fluxes, which represent up to 80-90% of terrestrial evapotranspiration (Jasechko et al., 2013), may affect the parental isotope composition of precipitation. Therefore, modern *d*-excess monitoring emerges as an imperative research effort to facilitate the interpretation of past climatic changes recorded in paleoclimatic archives. For example, Klein et al. (2015) observed a sharp *d*-excess decrease during a cyclone passing over the Arctic, deducing a change in RH over open water as the likely source of non-equilibrium evaporation on its path. Benetti et al. (2014) showed the negative correlation of *d*-excess and RH in continuous isotope measurement of water vapour during a 25-day period over the subtropical Eastern North Atlantic Ocean. Pfahl and Sodemann (2014) found that moisture source RH, and not SST, is the main driver of *d*-excess variability on seasonal time scales.

In the Central America region, paleoclimate studies based on stable isotope records have been limited. Lachniet et al. (2004a) suggested that enriched δ^{18}O values (up to -4 ‰) in Costa Rican stalagmite between ca. 8,300 to 8,000 yr B.P. were associated with reduced rainfall and a weaker monsoon in Central America, while depleted values (up to -7 ‰) were linked to a more stable monsoon regime, based on the well-known amount effect (monthly scale) rationale for tropical regions. Likewise, weaker monsoon regimes have been associated to an increased El Niño variability (Lachniet et al., 2004b). Pollock et al. (2016) suggested a slight increase and more stability in precipitation amounts during the mid-Holocene in Central America than present, based on δ^{18}O values from speleothems in Belize, using the same monthly precipitation amount rationale. Nevertheless, these paleoclimate interpretations should be re-evaluated in light of modern and high-resolution stable isotope data (i.e. long-term daily isotope data).

Isotopic composition has been regarded as a useful tool to analyze the evolution of the rain producing systems (Conroy et al., 2015) and changes within the boundary layer (Griffis et al., 2016). For instance, Aggarwal et al. (2016) proposed an alternative interpretation of subtropical and tropical isotope variability in precipitation focused on the distinction of rainfall generation mechanisms (i.e. deep convection versus stratiform rain fractions), which poses a new opportunity to analyze temporal and spatial isotopic variability in paleoclimatic records.

Here, we present a unique set of stable isotope data of daily precipitation collected prior to, during, and after a very strong El Niño event in Costa Rica, Central America, a region adversely affected by this phenomenon. Interannual and seasonal isotopic variations were analyzed in combination with air mass back trajectories and rain gauge data to understand ENSO effects on precipitation patterns linked to atmospheric moisture transport. Recent studies have demonstrated that variations in the stable isotope composition of precipitation even occur during storm events (Barras & Simmonds, 2009; Celle-Jeanton, Gonfiantini, Travi, & Sol, 2004; Coplen et al., 2008; Munksgaard, Wurster, Bass, & Bird, 2012), emphasizing the relevance of event-based and daily sampling in comparison with the modeling limitations offered by monthly stable isotope monitoring. To our knowledge, this is the first daily isotopic record in precipitation in the Intra-Americas Seas (i.e. an area of the tropical and subtropical western North Atlantic Ocean encompassing the Gulf of Mexico, the Caribbean Sea, the Bahamas and Florida, the northeast coast of South America, and the juxtaposed coastal regions, including the Antillean Islands; Maul, 2014), covering ENSO's neutral, warm, and the transition to a potential cold phase (La Niña). The present work also may contribute to understanding of groundwater recharge mechanisms in tropical regions where isotopically-informed geospatial models are becoming robust and common tools to improve water resources planification in a changing climate (Jasechko & Taylor, 2015; Sánchez-Murillo & Birkel, 2016; Taylor et al., 2013).

2 | CLIMATE GENERALITIES OF COSTA RICA DURING ENSO EVENTS

Costa Rica is located on the Central America Isthmus between 8° and 12°N latitude and 82° and 86°W longitude. Four regional air circulation processes predominantly control the climate of Costa Rica: NE trade winds, the latitudinal migration of the Intertropical Convergence Zone (ITCZ), cold continental outbreaks, and sporadic influence of tropical cyclones (Sáenz & Durán-Quesada, 2015; Waylen, Caviedes, & Quesada, 1996). Rainfall in the region is defined through the junction of the circulation and local features and processes that include topography, vegetation cover, and solenoid circulations. The interaction between large and local scale processes produces two predominant rainfall maxima, one in May-June and one in September-October. The rainfall maxima are interrupted by a relative minimum in July-August known as the Mid-Summer Drought (MSD) (Magaña, Amador, & Medina, 1999; Maldonado, Alfaro, Fallas-López, & Alvarado, 2013) that corresponds to a maximum in the Caribbean Low Level Jet (CLLJ) in July (i.e. a maximum of easterly zonal wind at 925 hPa in the Caribbean region; Amador, 1998, 2008; Herrera, Magaña, & Caetano, 2015). The development of deep convective systems is an important component of regional precipitation intensity and distribution. The diurnal cycle of precipitation offshore the Central American coast is largely forced by subsidence over land and offshore cloud movement linked with Mesoscale Convective Systems (MCS) activity (Janowiak, Kousky, & Joyce, 2005; Mapes, Warner, Xu, & Negri, 2003).

During El Niño, changes in the energy balance derived from differential warming between the northern and southern hemispheres causes the northward migration of the ITCZ. The shifting is more noticeable during boreal winter and is noticed as a southward shift of the ITCZ that can reach 5°S during strong El Niño events (Schneider, Bischoff, & Haug, 2014). The latitudinal shifting along with the longitudinal variation of the ITCZ due to re-organization of convection results in a decrease of deep convective activity and negative precipitation anomalies along the Pacific slope of Central America. The latter is a recurrent pattern particularly in the Dry Corridor of Central America (Cid-Serrano et al., 2015). Amador (2008) found that during warm ENSO phases, the CLLJ core is stronger, resulting in an increase of zonal easterly trade winds. Easterlies intensification decreases the moisture transport from the eastern Pacific Ocean and increases the transport of moisture from the Caribbean and northern South America (Durán-Quesada, 2012). A relevant aspect of regional precipitation is that unlike the Pacific domain, the Caribbean domain of Central America is wetter during the warm phase and drier during the cold phase (Cid-Serrano et al., 2015).

3 | DATA AND METHODS

3.1 | Combined El Niño 3.1/SOI Index

Monthly running average time series of the combined El Niño 3.4/SOI (Southern Oscillation Index) index were downloaded from the Earth System Research Laboratory of the National Oceanic and Atmospheric Administration (NOAA) (USA) (http://www.esrl.noaa.gov/psd/people/cathy.smith/best/enso.ts.1mn.txt) from January, 2013 to July 2016. This index combines an atmospheric component of the ENSO phenomenon (SOI) and an oceanic component (El Niño 3.4). Past SST values are often partially reconstructed. Therefore, by including the SOI, which is better measured historically, the effect of biases in the SST data introduced by the reconstruction methods are reduced and a better classification of the warm and cold phases can be obtained (Smith & Sardeshmukh, 2000).

3.2 | Precipitation collection and stable isotope analysis

Daily precipitation (N=280) was collected from March, 2013 to June, 2016 in central Costa Rica, Central America (Longitude: -84.1091; Latitude: 10.0004, Elevation: 1,173 m a.s.l.) using a passive collector (Palmex Ltd., Croatia) (Gröning et al., 2012). The site is located in the Central Valley of Costa Rica within the Pacific domain. A NW-SE cordillera (with maximum altitude of ~3,432 m a.s.l.) topographically divides the Pacific and Caribbean domains. We emphasize that to our knowledge there is no evidence of previous daily isotope records during a very strong El Niño event (e.g. 1982-83 and 1997-98) in the Intra-Americas Seas covering the entire ENSO evolution from neutral to a warm phase and the transition towards La Niña.

Samples were filtered using a Midisart PTFE (polytetrafluorethylene) 0.45 μm syringe membrane (Sartorius AG, Germany), transferred to 30 mL HDPE (high-density polyethylene) vials, and stored at 5°C until analysis. Stable isotope analysis was conducted at the Stable Isotope Research Group facilities of the National University of Costa Rica using a Cavity Ring Down Spectroscopy water isotope analyzer L2120-*i* (Picarro, USA). The secondary standards were: Moscow Tap Water, MTW (δ^2H = −131.4 ‰, δ^{18}O = −17.0 ‰), Deep Ocean Water, DOW (δ^2H = −1.7 ‰, δ^{18}O = −0.2 ‰), and Commercial Bottled Water, CAS (δ^2H = −64.3 ‰, δ^{18}O = −8.3 ‰). MTW and DOW standards were used to normalize the results to the VSMOW2-SLAP2 scale, while CAS was used as a quality control and drift control standard. The analytical long-term uncertainty was: ± 0.5 (‰) (1σ) for δ^2H, ± 0.1 (‰) (1σ) for δ^{18}O. The analytical uncertainty for *d*-excess (± 0.9 ‰) was estimated following Froehlich, Gibson, and Aggarwal (2001). Stable isotope compositions are presented in delta notation δ (‰, per mil), relating the ratios (R) of ^{18}O/^{16}O and ^{2}H/^{1}H, relative to Vienna Standard Mean Ocean Water (V-SMOW).

Simple linear regression analysis was performed to construct MWLs for each year. The amount weighted MWL of Costa Rica is presented as a reference (Sánchez-Murillo et al., 2013). Daily precipitation amounts (mm) were obtained from a Davis Vantage Pro2 Plus weather station installed next to the isotope passive collector. Stable isotope archives (N=679, 46 monitoring stations from 1993 to 2005) from the Global Network of Isotopes in Precipitation (GNIP; International Atomic Energy Agency/World Meteorological Organization, 2016) were used to compare long-term and recent *d*-excess values. A detailed description of the GNIP records for Costa Rica is presented in Sánchez-Murillo et al. (2013).

3.3 | HYSPLIT air mass back trajectories

The influence of atmospheric trajectory and source meteorological conditions on the subsequent stable isotope composition of precipitation was studied using the HYSPLIT Lagrangian model (Stein et al., 2015) developed by the Air Resources Laboratory (ARL) of NOAA (USA). The HYSPLIT model uses a three-dimensional Lagrangian air mass vertical velocity algorithm to determine the position of the air mass and reports these values at an hourly time-resolution over the trajectory (Soderberg et al., 2013). Air parcel trajectories were modeled 72 hours backwards in time based on the proximity of the Caribbean Sea and the Pacific Ocean. To compute a trajectory, the HYSPLIT model requires a starting time (13:00 p.m. UTC, which corresponds to the sample collection time of 7:00 a.m. in Costa Rica), location (-84.1091 W and 10.0004 N), and altitude (1,100 m a.s.l., Sánchez-Murillo et al., 2016a) as well as NOAA meteorological data files (e.g. GDAS, global data assimilation system: 2006-present; Su, Yuan, Fung, & Lau, 2015). In total, 280 air mass back trajectories were created and further divided into two main groups: the dry season (January-April) and the wet season (May-December). Following Klein et al. (2015), only the trajectories below one standard deviation of +5.5 (‰) in *d*-excess were selected. Since, historically, *d*-excess values in precipitation of Costa Rica are close to or above +10 (‰), the threshold selected was sufficient to conduct the moisture transport analysis.

3.4 | Precipitation and moisture anomaly diagnostics

Precipitation from the rain gauge network of the Costa Rica National Meteorological Institute was selected for two stations, Santa Lucía (Heredia, central Costa Rica, Pacific slope and same location as isotope precipitation sampling) and Limón (Caribbean slope). Data gaps were filled using the method by Alfaro and Soley (2009). Monthly precipitation anomalies were estimated based on the 1982-2012 normal period. Precipitation anomalies were normalized by the standard deviation of each month within the normal period.

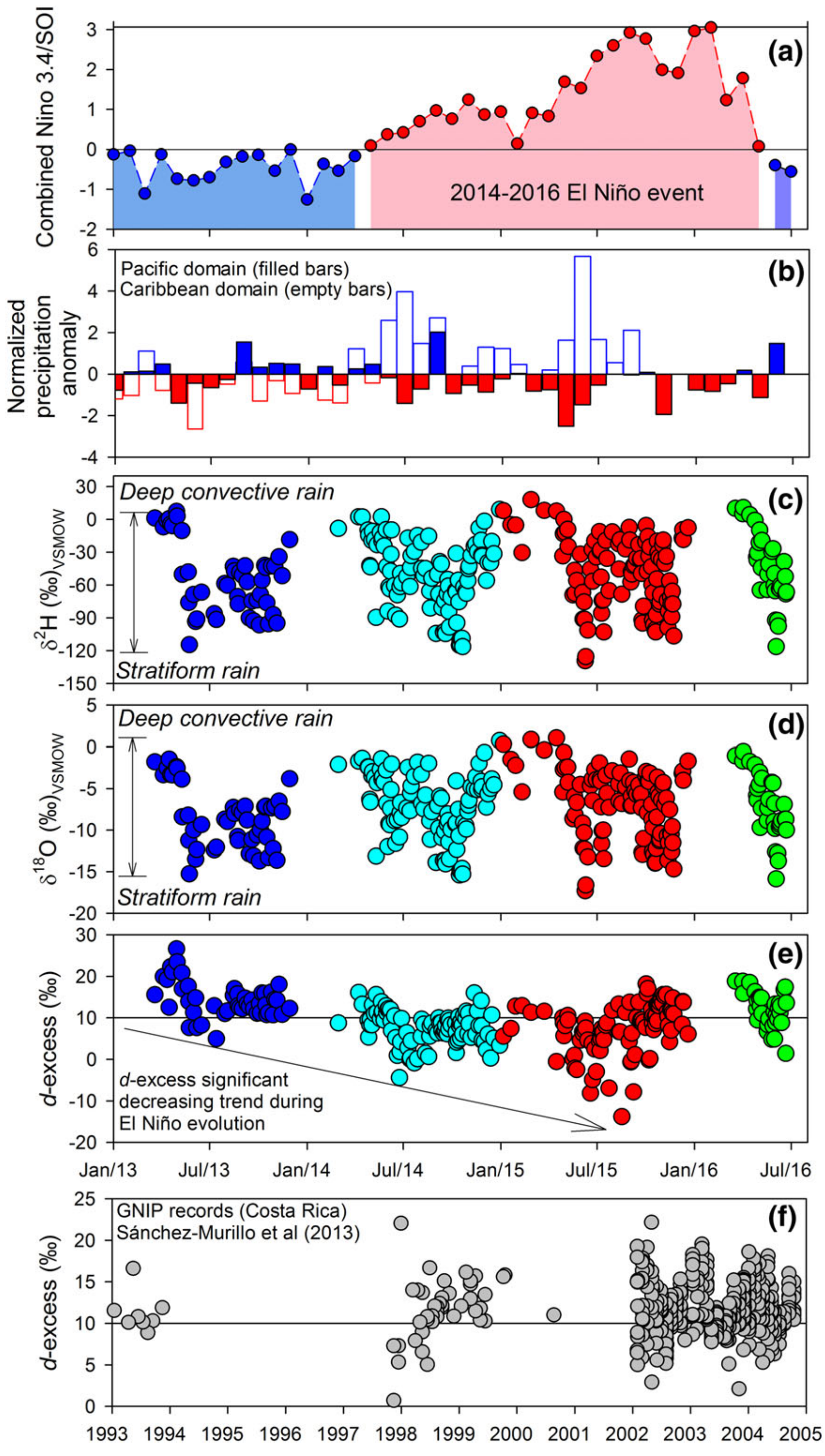

FIGURE 1 (a) ENSO combined Niño 3.4/SOI index time series (Smith & Sardeshmukh, 2000). (b) Normalized precipitation anomalies for the Pacific (filled bars) and Caribbean (empty bars) domains. (c) Daily δ^2H (‰) time series. (d) Daily δ^{18}O (‰) time series. The black arrows in C and D denote the differentiation between typically enriched convective rain versus more depleted stratiform rain following Aggarwal et al. (2016). (e) Daily *d*-excess (‰) times series showing (black arrow) a progressive and significant (P<0.001) decrease during the El Niño event. (f) Long-term monthly *d*-excess values from past-GNIP records in Costa Rica (Sánchez-Murillo et al., 2013). Years are color coded: 2013 (blue), 2014 (cyan), 2015 (red), and 2016 (green)

Daily Outgoing Longwave Radiation (OLR) was retrieved from the NCEP Reanalysis data provided by the NOAA/OAR/ESRL PSD, Boulder, Colorado (USA) (http://www.esrl.noaa.gov/psd/) (2.5 degrees resolution) to compute the anomalies for the recent El Niño episode using the same normal period (1982-2012) as for precipitation. A similar procedure was applied to ERA-Interim (0.75 degrees resolution) (Dee et al., 2011) monthly vertically integrated moisture flux divergence after extracting the convergence field.

3.5 | Statistical analysis

A Kruskal-Wallis non-parametric one way analysis of variance on ranks (Kruskal & Wallis, 1952) was applied to test if there was stochastically dominance of one year over another regarding $\delta^{18}O$ (‰), $\delta^{2}H$ (‰), and *d*-excess (‰) values. A significant difference was determined ($P<0.001$) when median values among the groups were greater than expected by chance. In addition, for all groups having a significant difference, an all pairwise multiple comparison procedure was applied using Dunn's method (Dunn, 1961) to test if there is evidence of stochastic dominance between the samples. Dunn's method approximates exact rank-sum test statistics by using the mean rankings of the results in each group from the previous Kruskal-Wallis non-parametric test and provides an inference in mean ranks in each group.

4 | INTERANNUAL AND SEASONAL ISOTOPIC VARIATIONS DURING EL NIÑO

In the 2013-2016 period, the largest SST anomalies were observed from January 2015 to May 2016 (Figure 1a), with a maximum anomaly

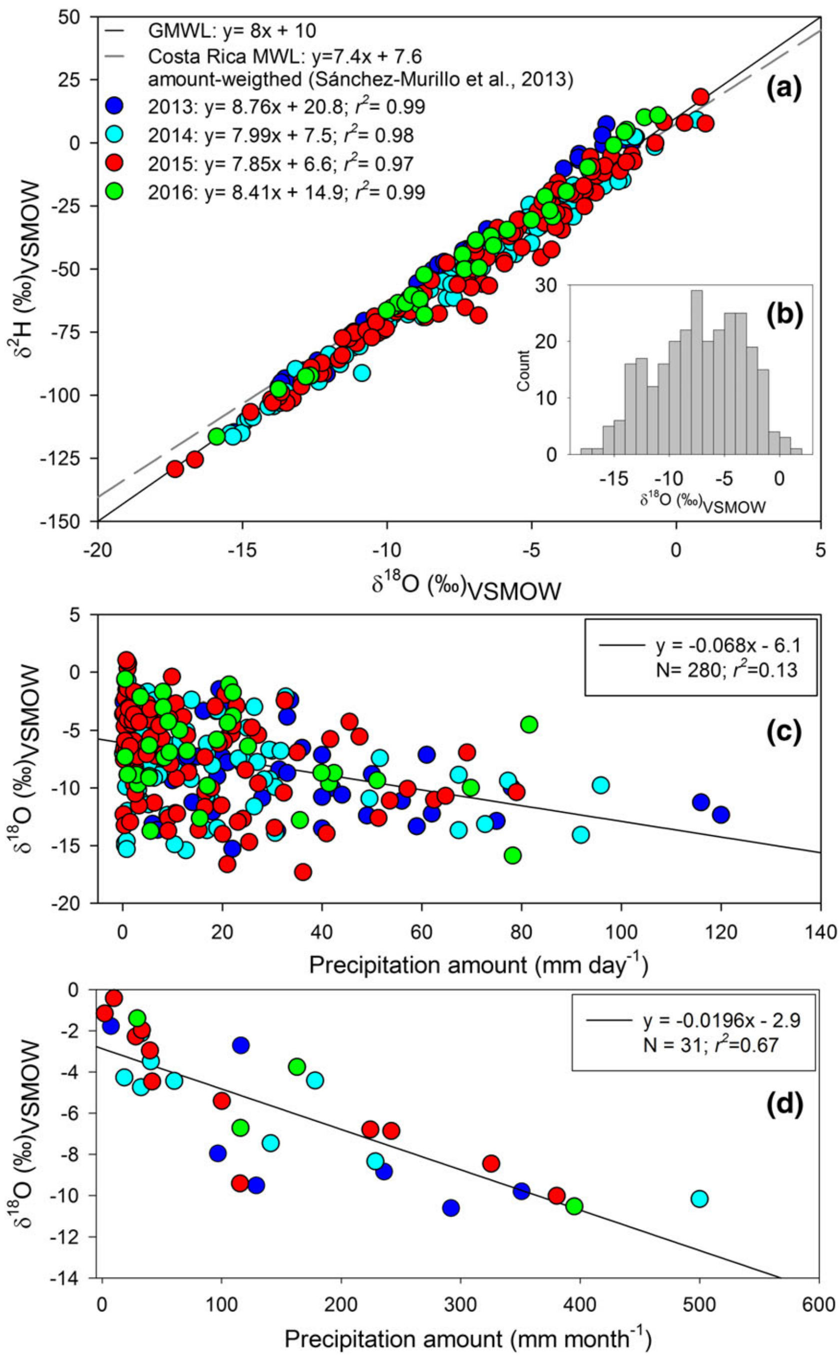

FIGURE 2 (a) Annual Meteoric Water Line regressions (MWLs) during El Niño event. The GMWL (black line) (Craig, 1961) and Costa Rican amount-weighted MWL (blue dashed line) (Sánchez-Murillo et al., 2013) are plotted for reference. (b) Histograms of all $\delta^{18}O$ (‰) values. (c) Linear relationship between daily $\delta^{18}O$ (‰) and daily precipitation amount (mm day^{-1}). (d) Linear relationship between monthly $\delta^{18}O$ (‰) and monthly precipitation amount (mm month^{-1}). Years are color coded: 2013 (blue), 2014 (cyan), 2015 (red), and 2016 (green)

peak in the September-October-November running average (+2.3°C) which is comparable only to two previous very strong events from 1982-83 (+1.9°C) and 1997-98 (+2.3°C) (NOAA, 2016). After almost eighteen months of a warm phase across the equatorial tropical Pacific Ocean, near-neutral conditions were observed during June-July, 2016 and La Niña is favored to develop during September-October-November, 2016 (NOAA, 2016). Figure 1b shows a comparison of normalized precipitation anomalies between the Pacific and Caribbean domains. During 2014-15, the precipitation deficit across the Pacific domain averaged 46% resulting in a very severe drought; while a 94% precipitation surplus was observed in the Caribbean domain.

Throughout the 2013-2016 period, δ^2H composition ranged from -129.4 up to +18.1 (‰) with an arithmetic mean of -49.4 ± 32.4 (‰) (1σ), while δ^{18}O composition varied from -17.3 up to +1.0 (‰) with an arithmetic mean of -7.3 ± 4.0 (‰) (1σ) (Figures 1c and 1d). Daily precipitation at the sampling site ranged from 0.2 mm to 120.0 mm with an arithmetic mean of 18.4 ± 21.5 mm (1σ). Transitions from dry (Jan-Apr) to wet season (May-Dec) were characterized by two clearly V-shaped patterns. Dry seasons were represented by enriched sporadic precipitation events (ranging from -1.6 to -3.3 ‰ δ^{18}O) (average precipitation amount: 7.4-13.9 mm day^{-1}). By mid-May, when the ITCZ passes over Costa Rica, a first notable depletion in isotope composition was observed (ranging from -12.0 to -17.3 ‰ δ^{18}O). This depletion pattern has also been reported in monthly GNIP archives for Costa Rica (Sánchez-Murillo et al., 2013) and in other regions of Central America (Lachniet, 2009; Lachniet & Paterson, 2009). Slight enrichment occurred during the transition of the MSD (July-August) (i.e. ITCZ northward migration ~8°N and development of deep convection over the Caribbean). Later in September and October, the isotopic composition exhibited a second strong depletion (ranging from -13.7 to -15.4 ‰ δ^{18}O) (Figures 1c and 1d) (average precipitation amount: 15.0-35.3 mm day^{-1}). As the ITCZ migrated southward by mid-November, a second enrichment was shown towards December and January. In general, dry season δ^2H and δ^{18}O ranged from -3.4 to -16.28 (‰) and -1.6 to -3.3 (‰), and wet season δ^2H and δ^{18}O ranged from -52.7 to -63.4 (‰) and -7.5 to -9.6 (‰), respectively.

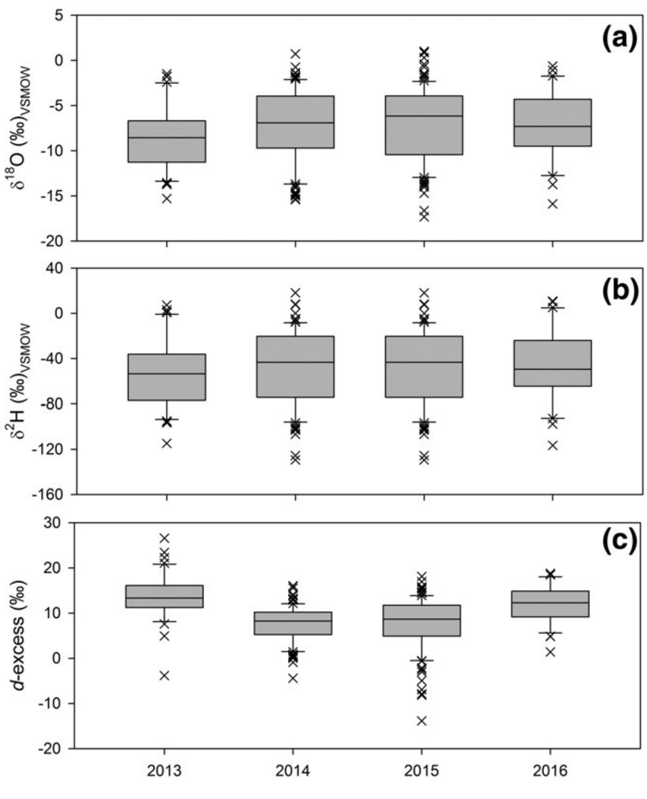

FIGURE 3 Distribution of δ^{18}O (‰) (a), δ^2H (‰) (b), and *d*-excess (‰) (c) from 2013-16. Box plots include median, 25*th* and 75*th* percentiles, and error bars. Crosses denote the number of outliers per sampling year. There was no statistically significant difference in *d*-excess (c) (‰) between 2013 and 2016; however *d*-excess medians were significantly different in 2014 and 2015 when compared to 2013 and 2016

The noticeable V-shaped patterns in Figures 1c and 1d were associated with the fluctuation of deep convective activity (i.e. small scale systems: 1-2 km and high intensity precipitation) and stratiform rain (i.e. large scale ~100 km and low intensity precipitation). Both convective and stratiform rain-types were also associated with the passage of MCS, when the type of rain is relative to the strength, position, and size of the systems as well as their area of influence. During the recent El Niño episode, the MCS activity was found to be reduced in the Pacific domain while it was enhanced in the Caribbean as clearly seen in the precipitation anomalies in Figure 1b. Therefore, precipitation changes due to the latest El Niño imply larger deep convection in the Caribbean, therefore an increase in heavy rainfall events; whereas deep convection in the Pacific was reduced and rainfall was mostly of the stratiform type. Aggarwal et al. (2016) found a negative correlation between isotopic composition and the stratiform rain fraction (SRF) (δ^{18}O= -0.20·SRF + 1.14; r^2=0.59, P<0.001) in tropical and mid-latitude regions. The author's isotope framework suggests that the Caribbean-Pacific rainfall contrast is intensified by the variation of rain producing systems and it should be reflected in depletion-enrichment patterns in both domains, as is in fact supported by the empirical evidence provided in Figures 1c and 1d and in various precipitation, groundwater, and surface water isoscapes recently presented by Sánchez-Murillo and Birkel (2016).

For example, enriched isotopic composition (ranging from +1 to -5 ‰ δ^{18}O) is a common feature of the Caribbean domain, corresponding to low stratiform fractions (<20%) dominated by shallow and deep convective activity based on the framework proposed by Aggarwal et al. (2016). In fact, these isotopic observations are in agreement with the storm characteristics for Costa Rica (i.e. based on the Tropical Rainfall Measuring Mission, TRMM) described by Rapp, Peterson, Frauenfeld, Quiring, and Roark (2014). The authors found that convective rains exceed stratiform rain during the boreal winter (Dec-Feb) and MSD (July-Aug), particularly in the Caribbean domain. This finding was supported by the enriched isotopic compositions observed (Figures 1c and 1d), whereas stratiform rain dominated the beginning and the end of the wet season (May-Nov) resulting in abrupt depletions in the Pacific domain. These sharp depletions were mainly observed in the Pacific slope of Central America (Sánchez-Murillo & Birkel, 2016) (-10 up to -15 ‰ in δ^{18}O) and were related to greater stratiform rain fractions (>60%), whereby ice formations above 0°C grow by vapour deposition with low δ^{18}O (Aggarwal et al., 2016). Precisely, during the El Niño evolution, the greater depletions were observed during 2015 (up to -17.3 ‰), which was represented by less intense precipitation episodes across the Pacific slope.

Temporal variation in *d*-excess showed that the lower values occurred during the warmest period of the El Niño event in 2015 (Figure 1e). Historical records from past GNIP stations in Costa Rica (Figure 1f) do not exhibit *d*-excess values below 0 (‰) among 46 stations, but rather represent local moisture recycling with *d*-excess values normally above +10 (‰). Overall, *d*-excess values ranged from +26.6 to -13.9 (‰) with an arithmetic mean of +9.2 ±5.5 (‰) (1σ). Dry and wet season *d*-excess means fluctuated from +8.51 up to +16.6 (‰) and +7.4 up to +13.3 (‰), respectively. The *d*-excess differences between neutral (2013), warm (2014-2015), and the beginning of a potential cold ENSO phase (2016) are well depicted in the annual meteoric water lines (MWLs) (Figure 2a). Both 2013 and 2016 exhibited similar MWLs with slopes and intercepts greater than 8 and 10, respectively. During the warmest El Niño phase (Figure 1a), however, there was a decrease for both slopes (7.9 – 7.8) and intercepts (7.5 – 6.6), differing from previous studies in central Costa Rica (Sánchez-Murillo & Birkel, 2016; Sánchez-Murillo et al., 2013, 2016a, 2016b). Typically, Costa Rican MWLs are on the order of 8.3-8.7 (slopes) and 11.2-20.7 (intercepts) and the Costa Rican amount-weighted MWL corresponds to $\delta^2H=7.4\delta^{18}O+7.6$ (Sánchez-Murillo et al., 2013). In general, isotope composition in precipitation of Central America exhibits a bi-modal distribution (Figure 2b) with one median between -5 and +1 (‰) for $\delta^{18}O$ (deep convective Caribbean-type rain) and another one between -5 and -15 (‰) as a result of larger stratiform systems mainly over the Pacific domain. Such a pattern has recently been reported by Sánchez-Murillo and Birkel 2016a in a series of precipitation, groundwater, and surface water high resolution isoscapes (i.e. isotopic geospatial representations). Additionally, on a daily scale, there is no strong correlation between precipitation amount and $\delta^{18}O$ (r^2=0.13, Figure 2c), however, this relationship becomes stronger when computing monthly $\delta^{18}O$ composites versus monthly precipitation amount (r^2=0.67, Figure 2d), resulting in a decrease of -2.0 ‰ per 100 mm. In terms of $\delta^{18}O$ (P=0.0186) and δ^2H (P=0.664), there was no significant difference among the medians throughout the study period (Figure 3), although a relative enrichment trend was observed from 2013 ($\delta^{18}O$ median = -8.6 ‰) to 2015 ($\delta^{18}O$ median = -6.2 ‰) (Figures 3a and 3b). Nevertheless, a significant decreasing trend (P<0.001) in *d*-excess (Figure 3c) was observed. Medians ranged from +13.3 (‰) in 2013 to +8.7 (‰) in 2015, a relative increasing trend was observed during 2016 with a median of +12.3 (‰).

Part of the rationale (Dansgaard, 1964) behind the empirical 'amount effect' relies on the idea that isotopic equilibration with the enriched vapour below the cloud base is more complete with the small raindrops associated with light rains. Therefore, lighter rainfall events (i.e. lower volume) will favor isotopic exchange with surrounding moisture and are subject to a more effective secondary evaporation below the cloud base. This is definitely a relevant driver

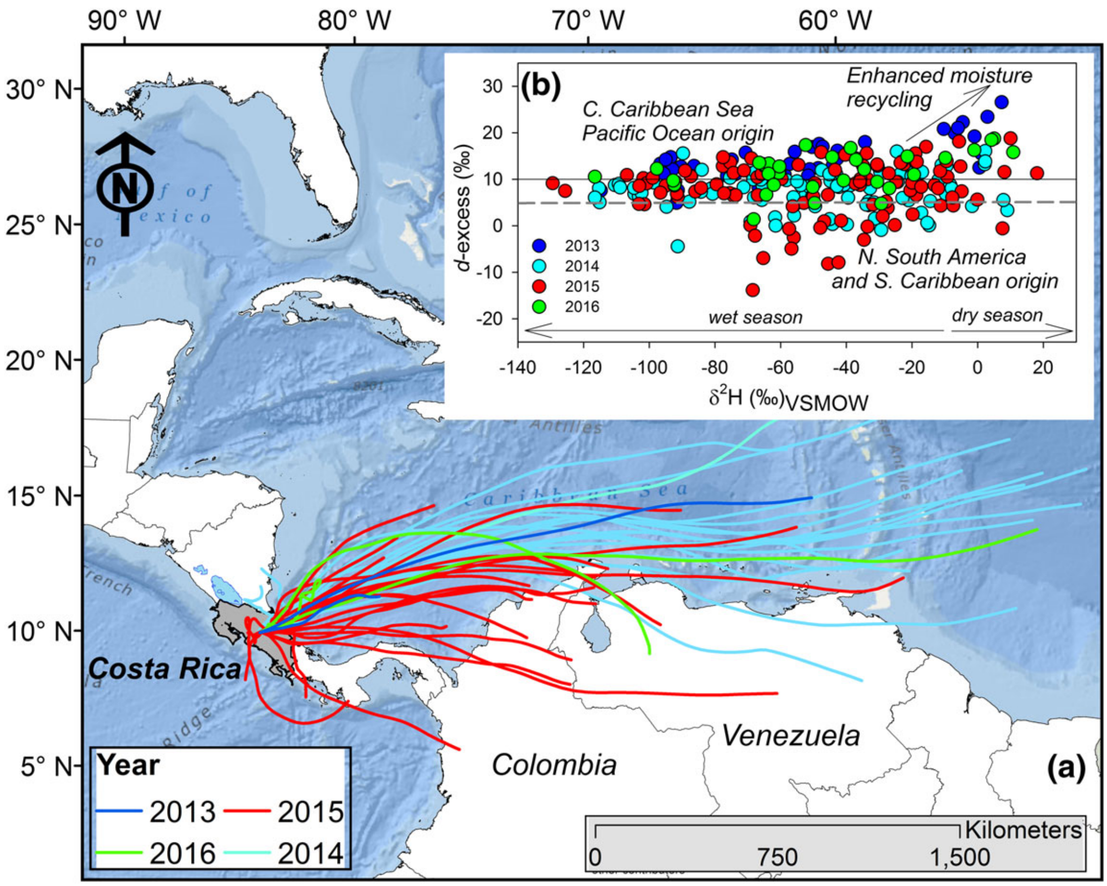

FIGURE 4 (a) Map of 72 (hr) air mass back trajectories exhibiting only *d*-excess values below 1σ (+5.5 ‰) following Klein et al., (2015). (b) Seasonal variation of all *d-excess* (‰) and δ^2H (‰) values during the El Niño 2014-16. The lower black arrows denote the separation between wet and dry seasons. The upper black arrow represents the increasing *d*-excess trend during the dry season. Three main groups are identified: i) maritime origin from the Pacific Ocean and central Caribbean Sea, ii) enhanced moisture recycling under large humidity gradients between the Pacific and Caribbean domains, and iii) northern South America and southeastern Caribbean origin. The horizontal black line represents a *d*-excess of +10 (‰) while the grey-dashed line denotes 1σ (+5.5 ‰). In both figures, years are color coded: 2013 (blue), 2014 (cyan), 2015 (red), and 2016 (green)

of *d*-excess changes in arid and semi-arid regions. In tropical regions, this could be the case in isolated rain events during the dry season when RH could be as low as 40-50%. However, during heavy rainfall events (i.e. large volume), RH below the cloud base is close to saturation and thus the moisture exchange is lower as well as the probability of secondary evaporation as water falls to the surface, which it decreases the likelihood of low *d*-excess as a response to below-cloud processes. The low *d*-excess values presented in this study occurred mainly during the wet seasons of El Niño 2014-16, therefore, the 'amount effect' relationship is no longer useful to explain the observed isotopic variations and an analysis of moisture source conditions was required.

5 | MOISTURE TRANSPORT AND *d*-excess CHANGES

Because of its unique geographical setting, Central America receives moisture inputs from the central and southeastern Caribbean Sea (primarily) and the Pacific Ocean when the easterly trade winds are weaker from September-November (Durán-Quesada, Gimeno, Amador, & Nieto, 2010; Sánchez-Murillo & Birkel, 2016). During the evolution of El Niño 2014-16, particularly during 2015, air mass back trajectories denoted a shift towards the incursion of southeastern Caribbean Sea (i.e. Lesser Antilles) moisture traveling mainly over the maritime region as well as moisture transport across the northern region of Colombia and Venezuela (Figure 4a). Systematic changes in moisture origin under distinct SST and RH conditions and the propagation of kinetic fractionation along the air mass trajectories have been recognized as potential drivers of *d*-excess changes (Jouzel et al., 2013; Klein et al., 2015). Using 72 (hr) air mass back trajectories for events with a *d*-excess below 1σ (+5.5 ‰) following Klein et al. (2015), a notable moisture transport pattern emerged. In 2013 and 2016 only five events (out of 78 daily events) exhibited a *d*-excess below +5.5 (‰), whereas in 2014 and 2015, 53 events (out of 198 daily events) presented lower values than +5.5 (‰). Figure 4b presents the relationship between all *d*-excess and δ^2H values, where three distinct groups can be identified: a) high *d*-excess values during the dry season (Jan-Apr) when moisture recycling is enhanced (i.e. local evapotranspiration) and favored by the intensification of the Pacific and Caribbean moisture gradient, b) maritime origin from the eastern Pacific Ocean and central Caribbean Sea which under warm ENSO

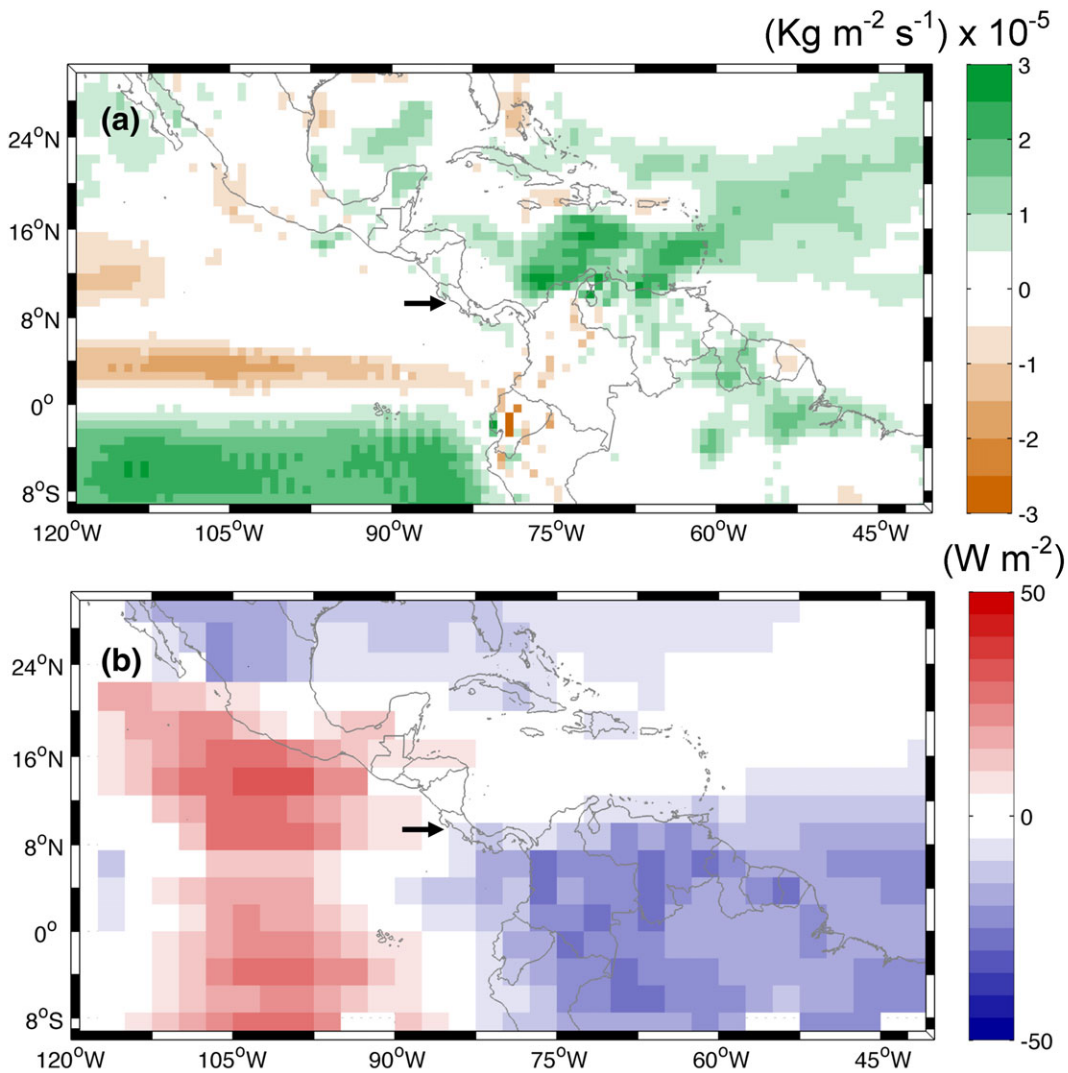

FIGURE 5 (a) Moisture flux convergence anomaly (kg m^{-2} s^{-1}, x 10^{-5}). (b) Outgoing Longwave Radiation anomaly (OLR) (W m^{-2}) during El Niño 2014-15 using the normal period of 1982-2012. The black arrow denotes the location of Costa Rica

conditions is featured by decreasing *d*-excess values. The intensification of the easterly flow modifies the moisture supply from the oceanic sources as the Caribbean Low Level jet acceleration redistributes local moisture uptake and transport, and c) anomalous low *d*-excess values of which air mass back trajectories indicate moisture transport from the southeastern Caribbean Sea (i.e. short lived over the sea trajectories), and moisture supply from the southeastern Caribbean Sea carried by the enhanced easterlies from western Venezuela (Figure 4a). During the recent El Niño, event moisture convergence was enhanced as shown by the green shaded area in Figure 5a. The intensification of the CLLJ increases local evaporation by surface drag and pulls moist air masses from the surroundings of the Maracaibo Lake as the pressure gradient is increased. The response of moisture transport from the Caribbean and northern South America under ENSO conditions was reported by Durán-Quesada (2012). The negative precipitation anomalies and systematic decrease of *d*-excess values are in good agreement with the large scale analysis that showed a strong reduction of the Pacific convective activity, meaning negative moisture flux convergence and positive OLR anomalies (red shaded area in Figure 5b). The opposite behavior is observed for the Caribbean domain. Warm ENSO conditions favor the intensification of convection as shown by the positive convergence anomalies (green shaded area in Figure 5a) and the corresponding negative OLR anomalies in Figure 5b. This pattern covers a large portion of the Pacific coast within the Dry Corridor of Central America (Figures 5a and 5b). However, enhanced convection (i.e., high relative humidity) was extended across the southern Caribbean Sea, the surrounding Atlantic Ocean, and in northern Colombia and Venezuela, the moisture source regions where low *d*-excess related trajectories originated (Figure 4b). This decreasing *d*-excess trend coupled with a notable suppression of convective activity across the Pacific coast of the Dry Corridor of Central America is the first recorded evidence (i.e. on a daily basis) of a very strong El Niño in modern isotope precipitation in the Intra-Americas Seas. Such signals provide novel information for future interpretation of past-ENSO events as well as the opportunity to re-analyze past interpretations in the light of a new regional circulation anomaly.

6 | CONCLUSIONS

This unique daily stable isotope data set in precipitation of Central America during ENSO's neutral, warm phase, and the transition to a potential cold phase revealed a significant decrease in mean annual *d*-excess values from +13.3 (‰) (2013) to +8.7 (‰) (2015), and a recovery at the start of the 2016 wet season (+12.3 ‰). Adverse El Niño impacts were observed for the Pacific (46% rain deficit causing a severe drought) and Caribbean (94% rain surplus causing severe floods) domains in Costa Rica. Particularly, changes in regional atmospheric circulation from commonly central Caribbean-type air mass trajectories to more southeastern Caribbean-type origin as well as moisture traveling across the Colombia and Venezuela region were associated with seasonal and interannual *d*-excess variations. The latter can be explained by an enhanced moisture flux convergence across the southeastern Caribbean Sea coupled with moisture transport from northern South America by means of an increased Caribbean Low Level Jet regime. The absence of significant differences in $\delta^{18}O$ and $\delta^{2}H$ during the evolution of this very strong El Niño event and the correspondence of *d*-excess values with the atmosphere-sea surface boundary conditions at the water vapour source, reinforce the applicability and suitability of *d*-excess as a reliable paleoclimatic proxy. By understanding past and modern ENSO dynamics, GCMs can be informed to improve precipitation forecasting across the tropics. Finally, further intra-event isotope sampling coupled with stratiform and convective fraction information is required to improve the understanding of tropical rain producing systems and their isotope-related variations.

ACKNOWLEDGMENTS

This project was supported by International Atomic Energy Agency grant CRP-19747 to RSM under the initiative “Stable isotopes in precipitation and paleoclimatic archives in tropical areas to improve regional hydrological and climatic impact models” and the Research Office of the National University of Costa Rica through grants SIA-0482-13, SIA-0378-14, and SIA-0101-14. The authors thank various helping hands that contributed to daily precipitation sampling at the Campus Omar Dengo of the National University of Costa Rica, Heredia, Costa Rica. CB acknowledges support from the University of Costa Rica (project 217-B4-239). Durán-Quesada acknowledges the projects VI-805-B3-600 and VI-805-B5-295 which provided the rain gauge data through a cooperation agreement with the Costa Rica National Meteorological Institute. Support from the Isotope Network for Tropical Ecosystem Studies (ISONet) funded by the University of Costa Rica Research Council is also acknowledged. Precipitation data was acquired through IMN-UCR agreement under VI-805-B3-600 and VI-805-B5-295 projects.

KEYPOINTS

- Unique daily isotope data set in tropical precipitation prior to, during, and after a very strong El Niño event
- Progressive and significant decrease of mean annual *d*-excess and precipitation amounts during El Niño evolution
- Lagrangian air mass back trajectories revealed a shift toward northern South America and southeastern Caribbean Sea moisture origin
- Identification of *d*-excess changes during modern strong El Niño events may improve paleoclimatic reconstruction in the Intra-Americas Seas

REFERENCES

Amador, J. A. (1998). A climatic feature of the tropical Americas: The trade wind easterly jet. *Tópicos meteorológicos y oceanográficos*, *5*(2), 91–102.

Amador, J. (2008). The intra-Americas seas low-level jet (IALLJ): Overview and future research. *Annals of the New York Academy of Sciences*, *1146*, 153–188. doi:10.1196/annals.1446.012

Alfaro, E. J., & Soley, F. J. (2009). Descripción de dos métodos de rellenado de datos ausentes en series de tiempo meteorológicas. *Revista de Matemática: Teoría y Aplicaciones*, *16*(1), 60–75.

Aggarwal, P. K., Romatschke, U., Araguas-Araguas, L., Belachew, D., Longstaffe, F. J., Berg, P., … Funk, A. (2016). Proportions of convective and stratiform precipitation revealed in water isotope ratios. *Nature Geoscience*. doi:10.1038/ngeo2739

Barras, V., & Simmonds, I. (2009). Observation and modeling of stable water isotopes as diagnostics of rainfall dynamics over southeastern Australia. *Journal of Geophysical Research*, *114*(D23), D23308. doi:10.1029/2009JD012132

Benetti, M., Reverdin, G., Pierre, C., Merlivat, L., Risi, C., Steen-Larsen, H. C., & Vimeux, F. (2014). Deuterium excess in marine water vapor: Dependency on relative humidity and surface wind speed during evaporation. *Journal of Geophysical Research-Atmospheres*, *119*, 584–593. doi:10.1002/2013JD020535

Bershaw, J., Saylor, J. E., Garzione, C. N., Leier, A., & Sundell, K. E. (2016). Stable Isotope Variations (δ18O and δD) in Modern Waters Across the Andean Plateau. *Geochimica et Cosmochimica Acta*, *194*(1), 310–324. doi:10.1016/j.gca.2016.08.011

Capotondi, A., Wittenberg, A. T., Newman, M., Di Lorenzo, E., Yu, J., Braconnot, P., … Yeh, S. (2015). Understanding ENSO Diversity. *Bulletin of the American Meteorological Society*, *96*, 921–938. doi:10.1175/BAMS-D-13-00117.1

Celle-Jeanton, H., Gonfiantini, R., Travi, Y., & Sol, B. (2004). Oxygen-18 variations of rainwater during precipitation: application of the Rayleigh model to selected rainfalls in Southern France. *Journal of Hydrology*, *298*, 165–177. doi:10.1016/j.jhydrol.2003.11.017

Cid-Serrano, L., Ramírez, S. M., Alfaro, E. J., & Enfield, D. B. (2015). Analysis of the Latin American west coast precipitation predictability using an ENSO index. *Atmosfera*, *28*(3), 191–203.

Craig, H. (1961). Isotopic variations in meteoric waters. *Science*, *133*(3465), 1702–1703. doi:10.1126/science.133.3465.1702

Coplen, T., Neiman, P., White, A., Landwehr, J. M., Ralph, F. M., & Dettinger, M. D. (2008). Extreme changes in stable hydrogen isotopes and precipitation characteristics in a landfalling Pacific storm. *Geophysical Research Letters*, *35*, L21808. doi: 10.1029/2088GL035481.

Dansgaard, W. (1964). Stable isotopes in precipitation. *Tellus*, *16*, 436–468. doi:10.1111/j.2153-3490.1964.tb00181.x

Dee, D. P., Uppala, S. M., Simmons, A. J., Berrisford, P., Poli, P., Kobayashi, S., … Vitart, F. (2011). The ERA-Interim reanalysis: configuration and performance of the data assimilation system. *Quarterly Journal of the Royal Meteorological Society*, *137*, 553–597. doi:10.1002/qj.828

Demény, A., Czuppon, G., Siklósy, Z., Leél-Őssy, S., Lin, K., Shen, C. C., & Gulyás, K. (2013). Mid-Holocene climate conditions and moisture source variations based on stable H, C and O isotope compositions of speleothems in Hungary. *Quaternary International*, *293*, 150–156. doi:10.1016/j.quaint.2012.05.035

Dittmann, A., Schlosser, E., Masson-Delmotte, V., Powers, J. G., Manning, K. W., Werner, M., & Fujita, K. (2016). Precipitation regime and stable isotopes at Dome Fuji, East Antarctica. *Atmospheric Chemistry and Physics*, *16*, 6883–6900. doi:10.5194/acp-2015-1012

Dunn, O. J. (1961). Multiple comparisons among means. *Journal of the American Statistical Association*, *56*(293), 52–64.

Durán-Quesada, A. M., Gimeno, L., Amador, J. A., & Nieto, R. (2010). Moisture sources for Central America: identification of moisture sources using a Lagrangian analysis technique. *Journal of Geophysical Research*, *115*(D05103). doi:10.1029/2009JD012455

Durán-Quesada, A. M. (2012). *Sources of moisture for Central America and transport based on a Lagrangian approach: variability, contributions to precipitation and transport mechanisms*. PhD Thesis, University of Vigo, Spain. 288 pp. [Available at http://www.investigo.biblioteca.uvigo.es/xmlui/handle/11093/267]

Food and Agriculture Organization of the United Nations. (2016). *El Niño and La Niña: preparedness and response, situation report July 2016*. [Available at http://www.fao.org/fileadmin/user_upload/emergencies/docs/FAOElNinoSitRep_versionJULY.pdf, accessed on August 12th, 2016.]

Frankenberg, C., Wunch, D., Toon, G., Risi, C., Scheepmaker, R., Lee, J. E., … Worden, J. (2013). Water vapor isotopologue retrievals from high-resolution GOSAT shortwave infrared spectra. *Atmospheric Measurement Techniques*, *6*(2), 263–274.

Froehlich, K., Gibson, J. J., & Aggarwal, P. (2001). Deuterium excess in precipitation and its climatological significance. In *Study of Environmental Change Using Isotope Techniques. Proc. Intern. Conf*. (pp. 54–66). Vienna, Austria.

Griffis, T. J., Wood, J. D., Baker, J. M., Lee, X., Xiao, K., Chen, Z., … Nieber, J. (2016). Investigating the source, transport, and isotope composition of water vapor in the planetary boundary layer. *Atmospheric Chemistry and Physics*, *16*(8), 5139–5157. doi:10.5194/acp-16-5139-2016

Good, S. P., Noone, D., Kurita, K., Benetti, M., & Bowen, G. J. (2015). D/H isotope ratios in the global hydrologic cycle. *Geophysical Research Letters*, *42*, 5042–5050. doi:10.1002/2015GL064117

Gröning, M. H., Lutz, O., Roller-Lutz, Z., Kralik, M., Gourcy, L., & Pöltenstein, L. (2012). A simple rain collector preventing water re-evaporation dedicated for δ18O and δ2H analysis of cumulative precipitation samples. *Journal of Hydrology*, *448*, 195–200. doi:10.1016/j.jhydrol.2012.04.041

Haese, B., Werner, M., & Lohmann, G. (2013). Stable water isotopes in the coupled atmosphere-land surface model ECHAM5-JSBACH. *Geoscientific Model Development*, *6*, 1463–1480. doi:10.5194/gmd-6-1463-2013

Hepp, J., Tuthorn, M., Zech, R., Mügler, I., Schlütz, F., Zech, W., & Zech, M. (2015). Reconstructing lake evaporation history and the isotopic composition of precipitation by a coupled δ18O–δ2H biomarker approach. *Journal of Hydrology*, *529*, 622–631. doi:10.1016/j.jhydrol.2014.10.012

Herrera, E., Magaña, V., & Caetano, E. (2015). Air–sea interactions and dynamical processes associated with the midsummer drought. *International Journal of Climatology*, *35*, 1569–1578. doi:10.1002/joc.4077

Hidalgo, H. G., Amador, J. A., Alfaro, E. J., & Quesada, B. (2013). Hydrological climate change projections for Central America. *Journal of Hydrology*, *495*, 94–112. doi:10.1016/j.jhydrol.2013.05.004

Hidayat, R., Ando, K., Masumoto, Y., & Luo, J. J. (2016). Interannual Variability of Precipitation over Indonesia: Impacts of ENSO and IOD and Their Predictability. *In IOP Conference Series: Earth and Environmental Science*, *31*(1), 012043. doi:10.1088/1755-1315/31/1/012043

Janowiak, J. E., Kousky, V. E., & Joyce, R. J. (2005). Diurnal cycle of precipitation determined from the CMORPH high spatial and temporal resolution global precipitation analyses. *Journal of Geophysical Research-Atmospheres*, *110*(D23105). doi:10.1029/2005JD006156

Jasechko, S., Sharp, Z. D., Gibson, J., Birks, S. J., Yi, Y., & Fawcett, P. J. (2013). Terrestrial water fluxes dominated by transpiration. *Nature*, *496*(7445), 347–350. doi:10.1038/nature11983

Jasechko, S., & Taylor, R. G. (2015). Intensive rainfall recharges tropical groundwaters. *Environmental Research Letters*, *10*(12), 124015. doi:10.1088/1748-9326/10/12/124015

Jouzel, J., Delaygue, G., Landais, A., Masson-Delmotte, V., Risi, C., & Vimeux, F. (2013). Water isotopes as tools to document oceanic sources of precipitation. *Water Resources Research*, *49*, 7469–7486. doi:10.1002/2013WR013508

Klein, E. S., Cherry, J. E., Young, J., Noone, D., Leffler, A. J., & Welker, J. M. (2015). Arctic cyclone water vapor isotopes support past sea ice retreat recorded in Greenland ice. *Scientific Reports*, *5*, 10295. doi:10.1038/srep10295

Klein, E. S., Nolan, M., McConnell, J., Sigl, M., Cherry, J., Young, J., & Welker, J. M. (2016). McCall Glacier record of Arctic climate change: Interpreting a northern Alaska ice core with regional water isotopes. *Quaternary Science Reviews*, *131*, 274–284. doi:10.1016/j.quascirev.2015.07.030

Kruskal, W. H., & Wallis, W. A. (1952). Use of ranks in one-criterion variance analysis. *Journal of the American Statistical Association*, *47*(260), 583–621.

Kusangaya, S., Toucher, M. L. W., van Garderen, E. A., & Jewitt, G. P. (2016). An evaluation of how downscaled climate data represents historical precipitation characteristics beyond the means and variances. *Global and Planetary Change*, *144*, 129–141. doi:10.1016/j.gloplacha.2016.07.014

Lachniet, M. S., Burns, S. J., Piperno, D. R., Asmeron, Y., Polyak, V. J., Moy, C. M., & Christenson, K. (2004a). A 1500-year El Niño/Southern Oscillation and rainfall history for the isthmus of Panama from speleothem calcite. *Journal of Geophysical Research-Atmospheres*, *109*(D20). doi:10.1029/2004JD004694

Lachniet, M. S., Asmerom, Y., Burns, S. J., Patterson, W. P., Polyak, V. J., & Seltzer, G. O. (2004b). Tropical response to the 8200 yr BP cold event? Speleothem isotopes indicate a weakened early Holocene monsoon in Costa Rica. *Geology*, *32*(11), 957–960. doi:10.1130/G20797.1

Lachniet, M. (2009). Sea surface temperature control on the stable isotopic composition of rainfall in Panama. *Geophysical Research Letters*, *36*, L03701. doi:10.1029/2008GL036625.L03701

Lachniet, M., & Paterson, W. (2009). Oxygen isotope values of precipitation and surface waters in northern Central America (Belize and Guatemala) are dominated by temperature and amount effects. *Earth and Planetary Science Letters*, *284*, 435–446. doi:10.1016/j.epsl.2009.05.010

Lee, J. E., Risi, C., Fung, I., Worden, J., Scheepmaker, R. A., Lintner, B., & Frankenberg, C. (2012). Asian monsoon hydrometeorology from TES and SCIAMACHY water vapor isotope measurements and LMDZ simulations: Implications for speleothem climate record interpretation. *Journal of Geophysical Research*, *117*(D15112). doi:10.1029/2011JD017133

Magaña, V., Amador, J. A., & Medina, S. (1999). The midsummer drought over Mexico and Central America. *Journal of Climate*, *12*(1967), 1577–1588. doi:10.1175/1520-0442(1999)012<1577:TMDOMA>2.0.CO;2

Maldonado, T., Alfaro, E., Fallas-López, B., & Alvarado, L. (2013). Seasonal prediction of extreme precipitation events and frequency of rainy days over Costa Rica, Central America, using Canonical Correlation Analysis. *Advances in Geosciences*, *33*(33), 41–52. doi:10.5194/adgeo-33-41-2013

Mapes, B. E., Warner, T. T., Xu, M., & Negri, A. J. (2003). Diurnal patterns of rainfall in northwestern South America. Part I: Observations and context. *Monthly Weather Review*, *131*(5), 799–812. doi:10.1175/1520-0493(2003)131<0799:DPORIN>2.0.CO;2

Maul, G. (2014). *Intra-Americas Sea. In Access Science*. McGraw-Hill Education. 10.1036/1097-8542.757445

Midhun, M., & Ramesh, R. (2016). Validation of δ18O as a proxy for past monsoon rain by multi-GCM simulations. *Climate Dynamics*, *46*, 1371. doi:10.1007/s00382-015-2652-8

Munksgaard, N. C., Wurster, C. M., Bass, A., & Bird, M. I. (2012). Extreme short-term stable isotope variability revealed by continuous rainwater analysis. *Hydrological Processes*, *26*, 3630–3634. doi:10.1002/hyp.9505

National Ocean and Atmospheric Administration. (2016). *ENSO cold and warm episodes by season*. Climate Prediction Center. Maryland, USA. [Available at http://www.cpc.ncep.noaa.gov/products/analysis_monitoring/ensostuff/ensoyears_ERSSTv3b.shtml, accessed on August 23rd, 2016.]

NOAA/OAR/ESRL PSD. *NCEP Reanalysis data*. Boulder, Colorado, USA. [Available at http://www.esrl.noaa.gov/psd/, accessed on August 20th, 2016.]

Nicholson, S. E. (2014). The Predictability of Precipitation over the Greater Horn of Africa. Part I: Prediction of Seasonal Precipitation. *Journal of Hydrometeorology*, *15*, 1011–1027. doi:10.1175/JHM-D-13-062.1

Pfahl, S., & Wernli, H. (2008). Air parcel trajectory analysis of stable isotopes in water vapor in the eastern Mediterranean. *Journal of Geophysical Research*, *113*(D20104). doi:10.1029/2008JD009839

Pfahl, S., & Sodemann, H. (2014). What controls deuterium excess in global precipitation? *Climate of the Past*, *10*, 771–778. doi:10.5194/cp-10-771-2014

Payne, V. H., Noone, D., Dudhia, A., Piccolo, C., & Grainger, R. G. (2007). Global satellite measurements of HDO and implications for understanding the transport of water vapour into the stratosphere. *Quarterly Journal of the Royal Meteorological Society*, *133*, 1459–1471. doi:10.1002/qj.127

Pollock, A. L., van Beynen, P. E., DeLong, K. L., Polyak, V., Asmerom, Y., & Reeder, P. P. (2016). A mid-Holocene paleoprecipitation record from Belize. *Palaeogeography*, *Palaeoclimatology*, *Palaeoecology*, *463*, 103–111. doi:10.1016/j.palaeo.2016.09.021

Rapp, A. D., Peterson, A. G., Frauenfeld, O. W., Quiring, S. M., & Roark, E. B. (2014). Climatology of Storm Characteristics in Costa Rica using the TRMM Precipitation Radar. *Journal of Hydrometeorology*, *15*, 2615–2633. doi:10.1175/JHM-D-13-0174.1

Risi, C., Landais, A., Winkler, R., & Vimeux, F. (2013). Can we determine what controls the spatio-temporal distribution of d-excess and 17O-excess in precipitation using the LMDZ general circulation model? *Climate of the Past*, *9*(2173). doi:10.5194/cp-9-2173-2013

Sáenz, F., & Durán-Quesada, A. M. (2015). A climatology of low level wind regimes over Central America using weather type classification approach. *Frontiers in Earth Science*, *3*(15), 1–18. doi:10.3389/feart.2015.00015

Sánchez-Murillo, R., Esquivel-Hernández, G., Welsh, K., Brooks, E. S., Boll, J., Alfaro-Solís, R., & Valdés-González, J. (2013). Spatial and temporal variation of stable isotopes in precipitation across Costa Rica: An analysis of historic GNIP records. *Open Journal of Modern Hydrology*, *3*(4), 226–240. doi:10.4236/ojmh.2013.34027

Sánchez-Murillo, R., & Birkel, C. (2016). Groundwater recharge mechanisms inferred from isoscapes in a complex tropical mountainous region. *Geophysical Research Letters*, *43*. doi:10.1002/2016GL068888

Sánchez-Murillo, R., Birkel, C., Welsh, K., Esquivel-Hernández, G., Corrales-Salazar, J., Boll, J., … Arce-Mesén, R. (2016a). Key drivers controlling stable isotope variations in daily precipitation of Costa Rica: Caribbean Sea versus Eastern Pacific Ocean moisture sources. *Quaternary Science Reviews*, *131*(Part B), 250–261. doi:10.1016/j.quascirev.2015.08.028

Sánchez-Murillo, R., Esquivel-Hernández, G., Sáenz-Rosales, O., Piedra-Marín, G., Fonseca-Sánchez, A., Madrigal-Solís, H., … Vargas-Víquez, J. A. (2016b). Isotopic composition in precipitation and groundwater in the northern mountainous region of the Central Valley of Costa Rica. *Isotopes in Environmental and Health Studies*. doi:10.1080/10256016.2016.1193503

Schneider, T., Bischoff, T., & Haug, G. H. (2014). Migrations and dynamics of the intertropical convergence zone. *Nature*, *513*(7516), 45–53. doi:10.1038/nature13636

Smith, C. A., & Sardeshmukh, P. (2000). The Effect of ENSO on the Intraseasonal Variance of Surface Temperature in Winter. *International Journal of Climatology*, *20*, 1543–1557.

Soderberg, K., Good, S. P., O'Connor, M., Wang, L., Ryan, K., & Caylor, K. K. (2013). Using atmospheric trajectories to model the isotopic composition of precipitation in central Kenya. *Ecosphere*, *4*(3). doi:10.1890/ES12-00160.1

Stein, A. F., Draxler, R. R., Rolph, G. D., Stunder, B. J. B., Cohen, M. D., & Ngan, F. (2015). NOAA's HYSPLIT Atmospheric Transport and Dispersion Modeling System. *Bulletin of the American Meteorological Society*, *96*, 2059–2077. doi:10.1175/BAMS-D-14-00110.1

Su, L., Yuan, Z., Fung, J. C. H., & Lau, A. K. H. (2015). A comparison of HYSPLIT backward trajectories generated from two GDAS datasets. *Science of the Total Environment*, *506-507*, 527–537. doi:10.1016/j.scitotenv.2014.11.072

Sutanto, S. J., Hoffmann, G., Worden, J., Scheepmaker, R. A., Aben, I., & Röckmann, T. (2015). Atmospheric processes governing the changes in water isotopologues during ENSO events from model and satellite measurements. *Journal of Geophysical Research-Atmospheres*, *120*, 6712–6729. doi:10.1002/2015JD023228

Taylor, R. G., Todd, M. C., Kongola, L., Maurice, L., Nahozya, E., Sanga, H., & MacDonald, A. M. (2013). Evidence of the dependence of groundwater resources on extreme rainfall in East Africa. *Nature Climate Change*, *3*(4), 374–378. doi:10.1038/nclimate1731

Tedeschi, R. G., & Collins, M. (2016). The influence of ENSO on South American precipitation during austral summer and autumn in observations and models. *International Journal of Climatology*, *36*, 618–635. doi:10.1002/joc.4371

Waylen, P. R., Caviedes, C. N., & Quesada, M. E. (1996). Interannual variability of monthly precipitation in Costa Rica. *Journal of Climate*, *9*, 2606–2613. doi:10.1175/1520-0442(1996)009<2606:IVOMPI>2.0.CO;2

Wolter, K., & Timlin, M. S. (1998). Measuring the strength of ENSO events: How does 1997/98 rank? *Weather*, *53*, 315–324. doi:10.1002/j.1477-8696.1998.tb06408.x

Yoshimura, K., Frankenberg, C., Lee, J., Kanamitsu, M., Worden, J., & Röckmann, T. (2011). Comparison of an isotopic atmospheric general circulation model with new quasi-global satellite measurements of water vapor isotopologues. *Journal of Geophysical Research*, *116*(D19118). doi:10.1029/2011JD016035

Yoshimura, K. (2015). Stable Water Isotopes in Climatology, Meteorology, and Hydrology: A Review. *Journal of the Meteorological Society of Japan*, *93*(5), 513–533. doi:10.2151/jmsj.2015-036

Zhang, T., Yang, S., Jiang, X., & Zhao, P. (2016). Seasonal–Interannual Variation and Prediction of Wet and Dry Season Precipitation over the Maritime Continent: Roles of ENSO and Monsoon Circulation. *Journal of Climate*, *29*, 3675–3695. doi:10.1175/JCLI-D-15-0222.1

How to cite this article: Sánchez-Murillo R, Durán-Quesada A M, Birkel C, Esquivel-Hernández G, Boll J. Tropical precipitation anomalies and *d*-excess evolution during El Niño 2014-16. *Hydrological Processes* 2016. doi: 10.1002/hyp.11088